Mathematical Model and Geometrical Design Method of Noncircular Face Gear with Intersecting Axes

Dawei Liu (liudw@ysu.edu.cn)
Yanshan University https://orcid.org/0000-0002-8129-0585
Zhenzhen Lv
Yanshan University
Guohao Zhao
Yanshan University

Original Article

Keywords: Face gear, Noncircular gear, Meshing equation, Space pitch curve, Tooth surface model

Posted Date: August 26th, 2020

DOI: https://doi.org/10.21203/rs.3.rs-64834/v1

Version of Record: A version of this preprint was published at Proceedings of the Institution of Mechanical Engineers, Part C: Journal of Mechanical Engineering Science on April 7th, 2021. See the published version at https://doi.org/10.1177/0954406221990708.

Mathematical Model and Geometrical Design Method of Noncircular Face Gear with Intersecting Axes

Dawei Liu* Zhenzhen Lv GuoHao Zhao

College of Mechanical Engineering, Yanshan University, Qinhuangdao 066004

Abstract: In order to establish the design method of a noncircular face gear (NFG) with intersecting axes, the meshing theory of this gear is investigated based on the principle of space gear meshing. A generalized approach for designing closed pitch curve of the NFG with intersecting axes is proposed based on Fourier series. The mathematical model of the NFG generated by a shaper cutter is established. The fundamental design parameters of the gears are defined, with the principle for determining their values discussed. The results of simulation and experiment verify the feasibility of the novel transmission mechanism and the correctness of the mathematical model of NFG with intersecting axes.

Keywords: Face gear; Noncircular gear; Meshing equation; Space pitch curve; Tooth surface model

1 Introduction

Noncircular gears integrate the features of the gear and cam, which can transmit accurately non-uniform motion between two shafts. As a simple function generator, they can be used to replace the expensive servo system and sensors in many mechanical devices to achieve specific motion law, such as the generator of the pulsating blood flow [1], soft robot joint actuation mechanism [2], differential velocity vane pump [3], indexing mechanism [4], potted vegetable seeding transplanting mechanism with punching hole [5], speed variator [6], differential of off-road vehicles [7] etc. The use of noncircular gear in equipment not only significantly reduces the system cost, but also greatly improves the reliability of the products in bad operating environment. Noncircular gears have broad application prospect in mechanical motion control fields. It is of great significance to study the meshing theory of noncircular gear for its application.

Much work has been performed on the meshing theory of planar noncircular gears. Scholars utilized the ellipse, eccentric circle, limacon [8] and some complex function, such as spline curve [9] and Fourier series curve [10], to construct pitch curves of noncircular gears with different transmission rules. Furthermore, the deformed and high-order non-circular gears are investigated to achieve more complicated motion rules [11-13]. In actual application, it is hoped that the pitch curve of non-circular gear can be reversely calculated according to the required transmission ratio. However, the transmission ratio of non-circular gear must satisfy the harsh closed conditions. Thus, it is usually hard to construct the closed pitch curve according to the given transmission ratio. For this, Liu and Ren[14] proposed a compensation method for designing the closed noncircular gears satisfying drive rule in a certain part. In addition to the synthesis of the pitch curves, the generation of tooth surface is another key problem of the noncircular gears. Litvin et al. [15] expounded systematically geometry of elliptical gears with straight and helical teeth generated by the rack, shaper and hob respectively, which could provide theoretical basis for the design and manufacture of all the planar noncircular gear. The meshing theory of planar noncircular gears is relative perfect.

With the development of process technology and the increase of the requirement on intersecting shafts transmission, the space noncircular gears become a hot research topic gradually. Noncircular bevel gear is the earliest spatial gears transmitting variable rotational speed. Xia et al. [16] presented the meshing theory in polar coordinates and established the mathematical model of the tooth profile of the gears by a pair of conjugated crown racks. Further, they deduced the tooth profile equation of noncircular bevel gears with concave pitch curve generated by a bevel gear cutter [17]. For the high-order deformed elliptic bevel gears, Lin et al. [18] paid much attention to the transmission mode and the kinematic characteristics, while Figliolini and Angeles [19] focused on the synthesis of the pitch cones. On the basis of the geometric model, Lin and He [20] simulated the meshing behaviors of the noncircular bevel gears to acquire the contact features and transmission errors. It can be seen from the above studies that the mathematical model of the tooth profile of the noncircular bevel gears is complicated and it is hard to process the conjugated space tooth surfaces of the gears, which restricts their application to some extent.

By replacing the pinion by a planar noncircular gear in a face gear mechanism, Lin et al. proposed a new gear mechanism comprised of a planar noncircular gear and a conjugated face gear called curve face gear. They carried out a series of fruitful studies on the meshing theory of the new gears, including the transmission mode [21], geometric model [22], compound motion [23], contact features [24] and so on. For the curve face gear mechanism, the axial installation error of the planar noncircular gear has no effect on the transmission accuracy. Hence, the difficulties of installation and manufacture of the curve face gear are reduced greatly relative to the noncircular bevel gears.

To further reduce the design and processing difficulty of the space noncircular gear, we presented a new gear called noncircular face gear (NFG), which is conjugated with an ordinary cylindrical gear. The transmission principle of the NFG drive, the construction approach of its pitch curves and the generation of tooth profile are demonstrated in literature [25]. Moreover, considering the convenience of the eccentric wheel as the wheel blank

Corresponding author：Dawei Liu，College of Mechanical Engineering, Yanshan University, Email：liudw@ysu.edu.cn

of the new face gear, the meshing theory of the eccentric face gear is investigated, with the touching trajectory on the tooth surface, the contact ratio and transmission characteristics discussed [26]. Since there is only one noncircular gear in the new gear pair, the closure condition of the pitch curve can be simplified greatly. In theory, a closed pitch curve of the noncircular face gear can be constructed by any given periodic transmission ratio. On the other hand, failure will occur more easily on the pinion due to the less teeth. So the noncircular face gear mechanism has better interchangeability than the noncircular bevel gear or the curve face gear mechanism does.

However, the existing investigations only focused on the noncircular face gear with perpendicular shafts, which can not apply to those with arbitrary intersecting shafts. Thereby, the emphasis in this article is paid on the meshing theory of noncircular face gears with intersecting axes to build the generalized mathematical models. The pitch curves and the transmission ratio function of the noncircular face gear with intersecting axes are presented, with the tooth surface model established. The fundamental design parameters of the gear are defined and the design procedure of the parameters is given. Finally, through the simulation and experiment, the correctness of the mathematical model and the design method of the noncircular face gear are validated.

2 Pitch curve and transmission ratio of NFG

2.1 Pitch surface and pitch curve

The noncircular face gear (NFG) drive with intersecting axes is composed by a cylindrical gear and a noncircular face gear as shown in Fig. 1(a). The cylindrical gear is a straight involute gear, while the NFG has non-constant rotational radius and its teeth distribute on the end face of the gear. In Fig. 1(b), λ is referred to as the angle between the gear axes. Generally, the cylindrical gear is the driving gear. When it rotates at a constant speed, the NFG runs with a periodically time-varying velocity.

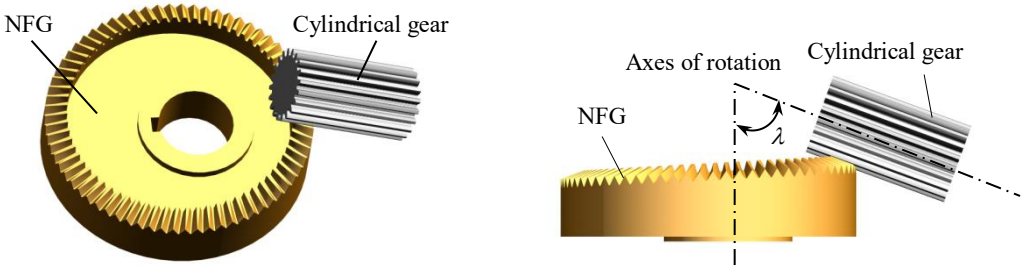

(a) axonometric drawing (b) Front drawing

Fig. 1 Noncircular face gear drive

The working pitch surface of the cylindrical gear is its reference cylinder in the case without installation error. Correspondingly, the pitch surface of the NFG is tangent to that of the cylindrical gear. When λ=90°, the pitch surface of the NFG is a plane. When $\lambda \neq$90°, it is a conical surface. Fig. 2 illustrates the pitch cone of the NFG and the pitch cylinder in a plane with $\lambda \neq$90°, in which the triangle and rectangle are the projections of the pitch cone and the pitch cylinder. Coordinate systems S_m and S_k are both fixed on the frame. The origin of S_m, O_m, is at the vertex of the pitch cone. z_m is the rotational axis of the NFG. The rotational axis of the cylindrical gear, z_k, intersects with z_m at O_k, which is the origin of coordinate system S_k. Axis y_k and axis y_m both perpendicular to plane $O_m x_m y_m$. The pitch cylinder is tangent to the pitch cone on their generatrix, $O_m M$, which is called the pitch line. Line $O_k I$ is the instantaneous rotation axis of the gears. The cross point P between lines $O_m M$ and $O_k I$ is specified pitch point. At point P, the two gears keep pure rolling. When the gears run, the trajectories of point P generate the pitch curves on the pitch surface of the two gears. The pitch curve of the NFG is a space noncircular curve on the pitch cone, while the pitch curve of the cylindrical gear is a spiral line on the pitch cylinder with non-constant helical pitch.

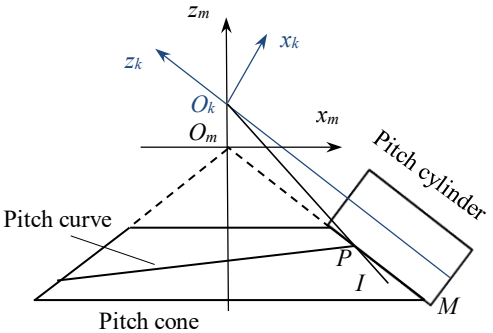

Fig. 2 Pitch surface and pitch curve

Coordinate system S_2 is fixed on the NFG. Fig. 3 illustrates the relationships of coordinate system S_2 and S_m. Origin O_2 and axis z_2 of coordinate systems S_2 coincide with origin O_m and axis z_m of coordinate system S_m respectively. ϕ_2 denotes the rotational angle of the NFG. The projection of the pitch curve of the NFG on plane

$O_2x_2y_2$ is a noncircular curve, whose radius vector and polar angle are r_2 and φ_2. When the gear start to rotation at φ_2=0, the polar angle is equal to the rotational angle of the NFG. For easy description, they are equivalent in the following content. Let the pitch circle radius of the cylindrical gear be R. The transmission ratio between the cylindrical gear and the NFG can be represented by

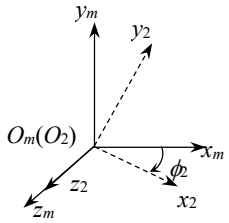

Fig. 3 Relationships between S_2 and S_m

$$i_{12}=\frac{\omega_1}{\omega_2}=\frac{r_2}{R} \tag{1}$$

where ω_1 and ω_2 denote rotational velocity of the cylindrical gear and the NFG respectively. Since r_2 varies with the rotation angle of the NFG, the NFG drive can transmit non-constant motion between two shafts.

2.2 Construction of pitch curve

In Eq. (1), R is a constant. The variable transmission ratio is determined by the pitch curve of the NFG uniquely, which is different from the ordinary noncircular gears. In the design of the NFG drive, we only need to construct the pitch curve of the NFG. When the rotational angle of the NFG is used as the independent variable, it will be very easy to construct a closed pitch curve of the NFG to obtain continuous transmission. The closure condition of the NFG is that the period of the transmission ratio is $2\pi/m$, where m represents the number of the NFG order. The transmission ratio of the NFG drive can be expressed as

$$i_{12}=\frac{\omega_1}{\omega_2}=i_j+\sum_{n=1}^{\infty}\left[a_n\cos(nm\varphi_2)+b_n\sin(nm\varphi_2)\right] \tag{3}$$

where $i_j=Z_2/Z_1$, Z_1 and Z_2 represent the number of teeth of the cylinder gear and the NFG respectively, m denotes the order of the pitch curve of the NFG, a_n and b_n are the coefficients of the transmission ratio. Substituting Eq. (3) into Eq. (1) could lead to the mathematical expression of the radius vector r_2. Then the formulae of the spatial pitch curve of the NFG can be represented as follows in coordinate system S_2:

$$\begin{cases} x_2=Ri_{12}\cos\varphi_2 \\ y_2=Ri_{12}\sin\varphi_2 \\ z_2=-Ri_{12}/\tan\lambda \end{cases} \tag{4}$$

If the independent variable of the transmission ratio of the NFG drive is the rotational angle of the cylindrical gear, φ_1. The transmission ratio function can be expressed as follows:

$$i_{21}=\frac{\omega_2}{\omega_1}=\frac{R}{r_2}=\frac{1}{i_j}+\sum_{n=1}^{\infty}\left[a_n\cos(\frac{nm\varphi_1}{i_j})+b_n\sin(\frac{nm\varphi_1}{i_j})\right] \tag{5}$$

For getting a closed pitch curve of the NFG, we only need to guarantee $i_j=z_2/z_1$ in Eq. (3) and Eq. (5). The other parameters, m, a_n and b_n, can be assigned any data. Eq. (3) and Eq. (5) could be used as generalized transmission ratio formulae for designing the closed pitch curve of the NFG.

3 Mathematical model of tooth surface of NFG

3.1 Enveloping theorem of NFG

Fig. 4 illustrates the generation of the NFG by a shaper cutter. Coordinate system S_2 is fixed on the NFG, which rotates around z_2. The rotational axis of the shaper is z_n. It intersects with axis z_2 at point O_n, which is the origin of the coordinate system S_n fixed on the frame. The angle between axis z_2 and axis z_n is λ, the shaft angle of the NFG drive. The shaper makes a reciprocating motion along axis z_n. Meanwhile the shaper and the NFG rotates with angular velocity ω_s and ω_2, which satisfy the following relationship

$$i_{s2}=\frac{\omega_s}{\omega_2}=\frac{r_2}{\rho} \tag{4}$$

where i_{s2} is the transmission ratio between the shaper and the NFG and ρ is the radius of the pitch circle of the shaper.

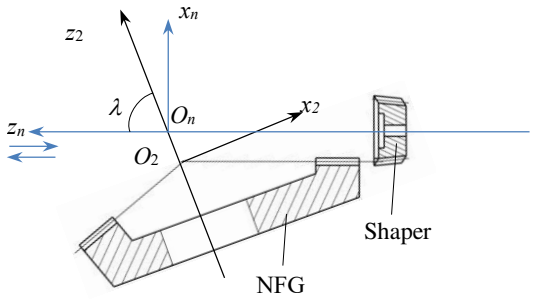

Fig. 4 Generation of the NFG by a shaper

If the number of teeth of the shaper is equal to that of the cylindrical gear, the NFG will contact with the cylindrical gear on lines in the engagement. It will lead to incorrect engagement easily due to the installation errors. Using for reference of the manufacture method of the circular face gear, we let the number of the shaper teeth be 1~3 more than that of the cylindrical gears. Then the NFG drive will make a point contact, which could reduce the adverse effect caused by the installation errors.

In Fig. 5 the shaper and the cylindrical gear make an imaginary inner gearing and they mesh with the NFG simultaneously. Coordinates system S_s and S_1 are fixed on the shaper and the cylindrical gear. R represents the pitch circle radius of the cylindrical gear. The tangent line between the pitch cylinder of the shaper and that of the cylindrical gear coincides with the pitch line O_mM in Fig. 2 and passes through the pitch point P on the pitch cone of the NFG.

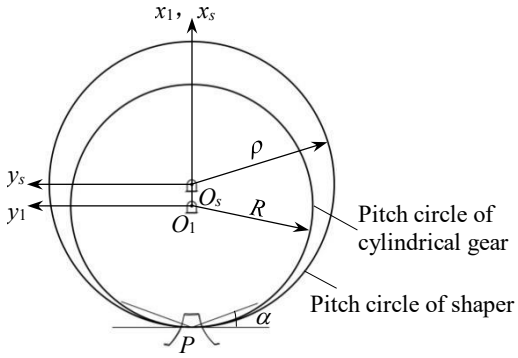

Fig. 5 Relationship between the shaper and the cylindrical gear

Fig. 6 shows a tooth of the shaper which meshes with the cylindrical gear and the NFG simultaneously. The contact line between the shaper and the cylindrical gear is a line parallel to their rotational axes, L_{s1}. The curve L_{s2} on the tooth surface of the shaper is the meshing line between the shaper and the NFG. The intersecting point Q between L_{s1} and L_{s2} is the contact point between the cylindrical gear and the NFG in practical engagement.

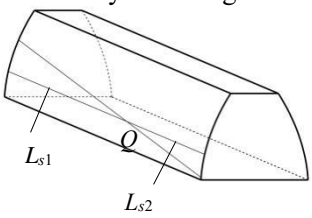

Fig. 6 Contacting lines on the tooth of the shaper cutter

3.2 Tooth surface model of the shaper

The tooth profile of the shaper is straight involute. In Fig. 7 r_{bs} denotes the radius of the base circle of the shaper. Line MN is the generating line of the involute. The phase angle of the starting point of the involute on the base circle is θ_q. The angle between line O_sM and line O_sN is θ_s. In coordinate system S_s, the model of the tooth profile of the shaper can be represented by

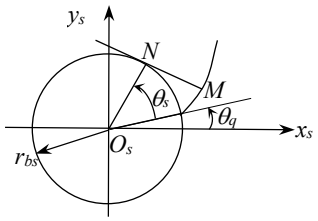

Fig. 7 Tooth profile of the shaper

$$\vec{r}_s(u_s,\theta_s)=\begin{bmatrix} x_s \\ y_s \\ z_s \\ 1 \end{bmatrix}=\begin{bmatrix} r_{bs}\theta_s\sin\left(\theta_s+\theta_q\right)+r_{bs}\cos(\theta_s+\theta_q) \\ \mp[r_{bs}\sin\left(\theta_s+\theta_q\right)-r_{bs}\theta_s\cos(\theta_s+\theta_q)] \\ u_s \\ 1 \end{bmatrix} \tag{5}$$

Here, u_s is the coordinate of the tooth profiles on axis z_s, and $\theta_q=\frac{\pi(N_s-1)}{2Z_s}+\frac{\pi}{2Z_s}-inv\alpha_0$, where Z_s represents the number of teeth of the shaper, α_0 is the pressure angle of the shaper, and N_s denotes the tooth number with N_s =1, 2$\cdots Z_s$. In addition, the upper and lower signs in Eq. (5) represent the left and right tooth profiles of the shaper respectively. According to the differential geometry theory, the unit normal vector on the tooth profile of the shaper can be expressed by

$$\vec{n}_s=\begin{bmatrix} \mp\sin(\theta_s+\theta_q) \\ -\cos(\theta_s+\theta_q) \\ 0 \end{bmatrix} \tag{6}$$

where the upper and lower signs correspond to the left and right profiles respectively.

Introduce another assistant coordinates fixed on the frame, S_c. There are five coordinate systems used in the derivation of the tooth surface formula of the NFG in total, in which S_2 and S_s are moveable coordinate systems fixed on the NFG and the cylindrical gear respectively, S_m, S_c and S_n are fixed on the frame. Fig. 8(a) illustrates the pitch cone of the NFG, the pitch cylinder of the shaper and the three fixed coordinate systems in a plane. Axis z_m and axis z_n are the rotational axes of the NFG and the shaper, which intersect at point O_n. The angle between axis z_m and axis z_n is λ, which is the same as the angle between shafts of the cylindrical gear and the NFG. Axis x_m is parallel to axis z_c and the distance between them is $\rho/\sin\lambda$. Fig. 3, Fig. 8(b), Fig. 8 (c) and Fig. 8(d) show the relationships of the five coordinate systems in three-dimensional space.

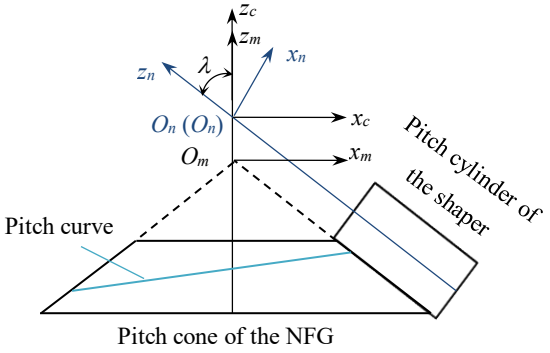

(a) Fixed coordinate systems in a plane

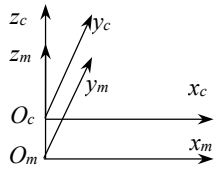

(b) S_m and S_c

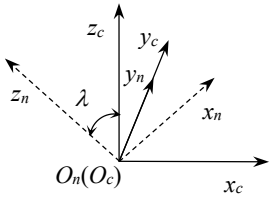

(c) S_c and S_n

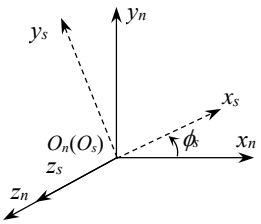

(d) S_n and S_s

Fig. 8 Relationships of coordinate systems

3.3 Meshing equation

According to the principle of gear meshing, the relative velocity between the cutting contact points on the tooth surfaces of two meshed gears is perpendicular to the common normal line on the points. The general formula of the meshing equation of gears is expressed by

$$f=\vec{N}^{(s)}\cdot\vec{v}^{(s2)}=0 \tag{7}$$

where $\vec{N}^{(s)}$ is the normal of the shaper tooth surface and $\vec{v}^{(s2)}$ is the relative velocity between the cutting contact points on the tooth surfaces. In the engagement of the cylindrical gear and the NFG, they still yield to the principle of gear meshing. We deduce the meshing equation of the NFG based on Eq. (7) below.

The meshing equation of the NFG is deduced in coordinate system S_s, where $\vec{N}^{(s)}$ can be represented by the unit normal vector, $\vec{n}_s$. Let the anticlockwise rotation velocity be positive. The rotation speed vector of the cylindrical gear in S_s is written by $\vec{\omega}_s^{s}=[0\ \ 0\ \ \omega_s]^{\mathrm{T}}$. The rotation speed vector of the NFG in S_c is written by $\vec{\omega}_c^{2}=[0\ \ 0\ \ -\omega_2]^{\mathrm{T}}$. By coordinate transformation we can get the rotation speed of the NFG in S_s as follows:

$$\vec{\omega}_s^{\,2}=M_{sc}\vec{\omega}_s^{\,2}=[-\cos\phi_s\sin\lambda\quad\sin\phi_s\sin\lambda\quad-\cos\lambda]^{\mathrm{T}} \tag{8}$$

where M_{sc} is the coordinate transformation matrix from S_c to S_s, and ϕ_s is the rotational angle of the shaper. The relative velocity between the tooth surfaces of the shaper and the NFG in S_s can be derived by the following equation

$$\vec{v}_s^{\,(s2)}=\left(\vec{\omega}_s^{s}-\vec{\omega}_s^{2}\right)\times\vec{r}_s=\omega_2\begin{bmatrix}z_s\sin\phi_s\sin\lambda+y_s\left(i_{s2}+\cos\lambda\right)\\-x_s\left(i_{s2}+\cos\lambda\right)+z_s\cos\phi_s\sin\lambda\\-x_s\sin\phi_s\sin\lambda-y_s\cos\phi_s\sin\lambda\end{bmatrix} \tag{9}$$

Substituting Eq. (6) and Eq. (9) into Eq. (7) leads to the meshing equation of the shaper and the NFG as follows:

$$f\left(u_s,\theta_s,\phi_s\right)=-u_s\sin\lambda\cos(\theta_q+\theta_s\mp\phi_s)+r_{bs}(i_{s2}+\cos\lambda)=0 \tag{10}$$

where the upper and lower sign correspond to the left and right tooth profile of the shaper.

3.4 Tooth surface model of the NFG

According to Eq. (10), we can get the function of parameter u_s as follows:

$$u_s=\frac{r_{bs}(i_{s2}+\cos\lambda)}{\sin\lambda\cos(\theta_q+\theta_s\mp\phi_s)} \tag{11}$$

Substituting Eq. (11) into Eq. (5) can result in the expression of the meshing line between the shaper and the NFG in coordinate system S_s as the following equation

$$\vec{r}_s(\theta_s,\phi_s)=\begin{bmatrix}r_{bs}\theta_s\sin\left(\theta_s+\theta_q\right)+r_{bs}\cos(\theta_s+\theta_q)\\\mp[r_{bs}\sin\left(\theta_s+\theta_q\right)-r_{bs}\theta_s\cos(\theta_s+\theta_q)]\\\dfrac{r_{bs}(i_{s2}+\cos\lambda)}{\sin\lambda\cos(\theta_q+\theta_s\mp\phi_s)}\\1\end{bmatrix} \tag{12}$$

Transforming the coordinates of the meshing lines from S_s to S_2 leads to the formula of the working tooth surface of the NFG as follows:

$$\vec{r}_2(\theta_s,\phi_s)=M_{2s}\vec{r}_s(\theta_s,\phi_s) \tag{13}$$

where M_{2s} is the coordinate transformation matrix from S_s to S_2, with

$$M_{2s}=\begin{bmatrix}\cos\phi_2\cos\lambda\cos\phi_s-\sin\phi_2\sin\phi_s & -\cos\phi_2\sin\phi_s\cos\lambda-\cos\phi_s\sin\phi_2 & -\sin\lambda\cos\phi_2 & 0\\\cos\lambda\sin\phi_2\cos\phi_s+\cos\phi_2\sin\phi_s & \cos\phi_s\cos\phi_2-\cos\lambda\sin\phi_2\sin\phi_s & -\sin\lambda\sin\phi_2 & 0\\\sin\lambda\cos\phi_s & -\sin\phi_s\sin\lambda & \cos\lambda & \rho/\sin\lambda\\0 & 0 & 0 & 1\end{bmatrix} \tag{14}$$

In Eq. (14), the rotation angles ϕ_2 and ϕ_s satisfy the following equation

$$\phi_2=\int_0^{\phi_s}\frac{1}{i_{s2}}d\phi_s \tag{15}$$

The fillets of the NFG are enveloped by the tooth tips of the shaper. In coordinate system S_s, the tooth tip can be expressed by $\vec{r}_s(u_s,\theta_s^*)$, where

$$\theta_s^*=\sqrt{r_{as}^{\,2}-r_{bs}^{\,2}}\,\Big/r_{bs} \tag{16}$$

Here, r_{as} is the radius of the tooth top circle of the shaper. The fillets of the NFG can be derived by transforming $\vec{r}_s(u_s,\theta_s^*)$ from S_s to S_2.

$$\vec{r}_2^{\,f}(u_s,\phi_s)=M_{2s}\vec{r}_s(u_s,\theta_s^*) \tag{17}$$

4 Geometric design of NFG

4.1 Basic design parameters

For the NFG drive, there are five basic design parameters like ordinary involute cylindrical gears, the module, number of teeth, pressure angle, addendum coefficient and tip clearance coefficient.

The module of the NFG on the pitch curve is equal to that of the cylindrical gear on the pitch circle. So we define the module of the cylindrical gear as the module of the NFG pair, which can be selected in the standard module series of involute gears.

Z_1 and Z_2 are specified the number of the teeth of the cylindrical gear and the NFG, which satisfy the equation $i_j = Z_2 / Z_1$. Generally, the transmission ratio of the NFG drive will be constructed by Eq. (3) and Eq. (5) firstly. Then according to the installation space and the operating requirement, we decide the number of teeth of the cylindrical gear. Finally, the number of teeth of the NFG can be derived by $Z_2 = Z_1 \ i_j$. Using the universal transmission ratio of Eq. (3) or Eq.(5), we can obtain a closed NFG as long as Z_1 and Z_2 are integers.

For involute cylindrical gears, the pressure angle is that on the pitch circle of the gears. The pressure angle of the NFG on the pitch cone is equal to that of the cylindrical gear. So the pressure angles of the two gears α_0 can be chosen from the standard pressure angle of involute gears.

The addendum coefficient and tip clearance coefficient of the NFG drive, h_a^* and c^*, are the same to those of the ordinary gears. For the NFG, the addendum is represented by $h_a = m\ h_a^*$, while the dedendum is expressed by $h_f = m\ (h_a^* + c^*)$. The addendum surface and dedendum surface are the normal isometric surfaces of the pitch cone one.

4.2 Tooth width

The pitch curve of the NFG, C_2, is a space curve on the pitch cone as shown in Fig. 9. The curves C_{2n} and C_{2w} are the inner and outer curve of the NFG teeth on the pitch cone. The distance between the inner curve and the pitch curve along the generator of the pitch cone is L_n, while the distance between the outer curve and the pitch curve is L_w. The tooth width of the NFG is expressed by $B_2 = L_w + L_n$. In the coordinate systems S_2, the inner and outer curve can be represented by

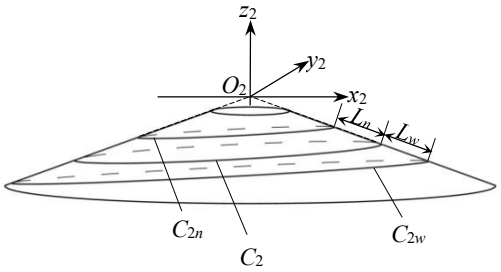

Fig. 9 Inner and outer curve of the teeth on the pitch cone

$$\begin{cases} x_2^{\,n} = (r_2 - L_n \sin\lambda)\cos\varphi_2 \\ y_2^{\,n} = (r_2 - L_n \sin\lambda)\sin\varphi_2 \\ z_2^{\,n} = -(r_2 - L_n \sin\lambda)/\tan\lambda \end{cases} \tag{18}$$

$$\begin{cases} x_2^{\,w} = (r_2 + L_w \sin\lambda)\cos\varphi_2 \\ y_2^{\,w} = (r_2 + L_w \sin\lambda)\sin\varphi_2 \\ z_2^{\,w} = -(r_2 + L_w \sin\lambda)/\tan\lambda \end{cases} \tag{19}$$

where the upper signs n and w correspond to the inner and outer curve of the teeth.

As we know, the undercutting and tip-cutting will appears on the tooth of the circular face gear if the tooth width exceeds a certain value. The same phenomenon occurs on the NFG. For circular face gear, the academic criterion of the undercutting and tip-cutting was presented in literature [27], with the maximal tooth width discussed. However, variable radius vector of the NFG brings large difficulty to deduce the academic criterion of the tooth shape imperfections. From machining simulation, we found that undercutting and tip-cutting appear more easily on the tooth where the radius vector is minimal [26]. Studies on circular face gear state that the limit width of the gears decreases as the face gear radius decreases too. So it can be concluded that the limit width of the NFG is decided by the minimum of the radius vector of its pitch curve, $r_{2\min}$. Near $r_{2\min}$, the transmission ratio of the NFG does not change much, where the tooth shape is similar to that of a circular face gear with $r_{2\min}$ as the radius of its pitch circle. Thereby, the circular face gear with radius $r_{2\min}$ is defined as the equivalent gear of the NFG, which is used to judge the undercutting and tip-cutting and calculate the limit width of the NFG. Literature [27] gives derivation of the limit width of the circular face gear in detail, which will not be repeated in this article.

It can be seen from Fig. 9 that the teeth of the NFG distribute along the pitch curve. For guaranteeing normal engagement of the NFG drive, the cylindrical gear must have the long enough tooth width. The minimum of the tooth width of the cylindrical gear can be written by

$$B_{1\min} = L_w + L_n + (r_{2\max} - r_{2\min})/\sin\lambda \tag{20}$$

where $r_{2\max}$ and $r_{2\min}$ are the maximum and minimum of r_2.

The process for designing the NFG drive is illustrated in Fig. 10. Firstly, the basic parameters of the

cylindrical gear need to be determined. Parameters α_0, h_a^* and c^* are assigned with the standard values of the involute spur gears. The crossed axis angle, l, is determined by the operating requirement of the gearing. m and Z_1 would be estimated with consideration of the installation space, empirical values and so on. Then the number of the teeth of the NFG is obtained by $Z_2=Z_1 i_j$. Otherwise, the pitch curve of the NFG is not closed. The minimal radius vector of the pitch curve of the NFG, $r_{2\min}$, is gained by the transmission ratio and pitch circle radius of the cylindrical gear of the NFG drive. According to the judgement rules of the undercutting and tip-cutting, the limit width of a circular face gear with radius $r_{2\min}$ can be calculated, which is used as the limit width of the NFG. Then, using Eq. (20), the minimum of the toot width of the cylindrical gear can be derived. Finally, the contact and bending stress of the NFG drive should be calculated to verify that the gears satisfy the strength requirement. If the requirement is not met, we need to adjust parameters m and Z_1, and recalculate others according to the design procedure in Fig. 10.

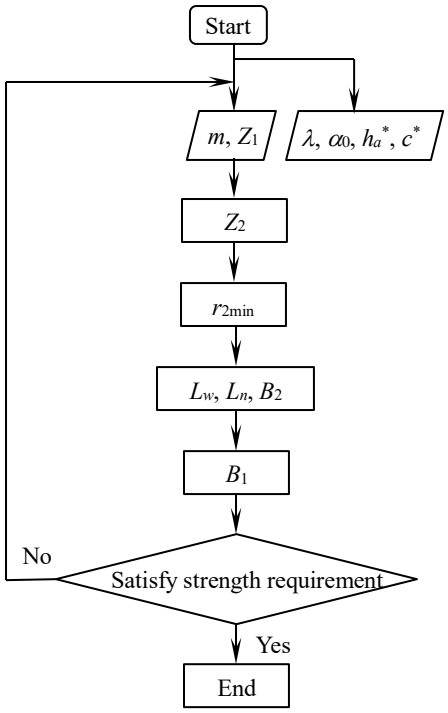

Fig. 10 Design flow of the NFG drive

5 Results and discussion

In this section, a design example of NFG with intersecting axes is given. An analysis of the transmission ratio characteristics of the NFG is made, with the effects of the design parameters on the transmission ratio discussed. Then two simulation models of the NFG are built by the proposed mathematical model and gear shaping simulation respectively, with the comparison between tooth surfaces made. Finally using the simulation model, the NFG is machined in a CNC machine center, with the practical transmission ratio tested. The first goal here is to demonstrate the transmission ratio rules, which can be used to determine or adjust the value of parameters in practical application. The second goal is the validation of the mathematical model and design method of the NFG with intersecting axes.

In the example, the first term harmonic in Eq. (5) is selected as the transmission ratio of a NFG drive. Setting $a_1= \varepsilon / i_j$, and $b_1 = 0$, we can get the simplest expression of the transmission ratio function as

$$i_{21}=\frac{1}{i_j}+\frac{\varepsilon}{i_j}\cos(m\frac{\varphi_1}{i_j}) \tag{21}$$

where ε represent the eccentric ratio of the NFG. The transmission ratio parameters are determined based on the application requirement. Here, set i_j=3.7, ε=0.5 and m=1.The basic design parameters of the NFG are given as shown in Table. 1, where the shaper cutter has one more teeth than the cylindrical gear does.

Table 1 Basic design parameters of a NFG

Parameter	Value
Average of the transmission ratio i_j	3.7
Eccentric ratio of the NFG ε	0.15
Order of pitch curve of the NFG m	1
Module of the gear m_s/mm	2

Number of teeth of the cylindrical gear Z_1	19
Pressure angle α_0/°	20
Addendum coefficient h_a^*	1
Tip clearance coefficient c^*	0.25
Angle between gears λ	80°
Number of teeth of the shaper Z_s	20
Number of teeth of the NFG Z_2	70

Following the design flow in Fig. 10, the maximum tooth width parameters of the NFG is calculated as $L_{w\max}$=10.1111 mm and $L_{n\max}$=3.8158 mm. Take L_w=10 mm and L_n=3.5 mm. The tooth width of the NFG is given by B_2 = 13.5mm. Using Eq. (20), we calculated that the minimal tooth width of the cylindrical gear is 41.287 mm. Eventually, we take the tooth width of the cylindrical gear as B_1 = 45 mm.

5.1 Transmission ratio characteristics

It is known from Eq. (21), the transmission ratio i_{21} comprises of the reduction ratio i_j and the variable transmission ratio i_b=1+ε cos($m\varphi_1$ / i_j). Hence, the NFG drive is equivalent to a serial gear mechanism composed of a pair of bevel or face gears and a pair of noncircular gears as shown in Fig. 11(a), where the reduction ratio of bevel gear is 3.7 and the noncircular gears behave according to the transmission ratio i_b shown in Fig. 11(b). In practice, the serial gear mechanism can be replaced by the NFG drive to reduce the weight and installation space of the transmission system greatly. This is very appropriate for the equipment which has strict demand on the weight and size, such as robots, instruments, aircraft and so on.

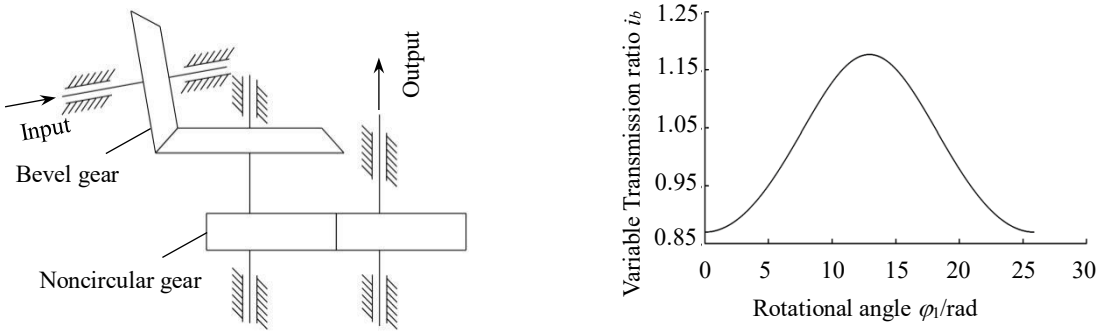

(a) Two-stage gear mechanism (b) Variable transmission ratio i_b

Fig. 11 Equivalent transmission mechanism of the NFG drive

In Eq. (21), there are three parameters, i_j, ε and m, to determine the transmission ratio of the NFG. Adjusting one of the three parameters independently and keeping the other parameters in Table 1 invariant, we draw the transmission ratio curves varying with φ_2 to analyze the effects of the three parameters on the transmission rules in Fig. 12. Define the transmission range of the gears as the ratio of the maximum to the minimum of the transmission ratio. The reduction ratio, transmission range and number of transmission ratio period are used to describe the features of the transmission rules of the NFG.

Set Z_1 as 17,18 and 19 respectively. Correspondingly, the values of the i_j are 4.1, 3.9 and 3.7. With the decrease of i_j, the transmission rule curves moves down along the vertical axis integrally in Fig. 12(a). However, the transmission range and number of transmission ratio period does not change with i_j. Similarly, when ε or m varies, one of the three transmission features of the NFG changes accordingly. The transmission range expands as ε increases in Fig. 12(b), while the period of the transmission ratio linearly increases with an increment of m in Fig. 12(c).

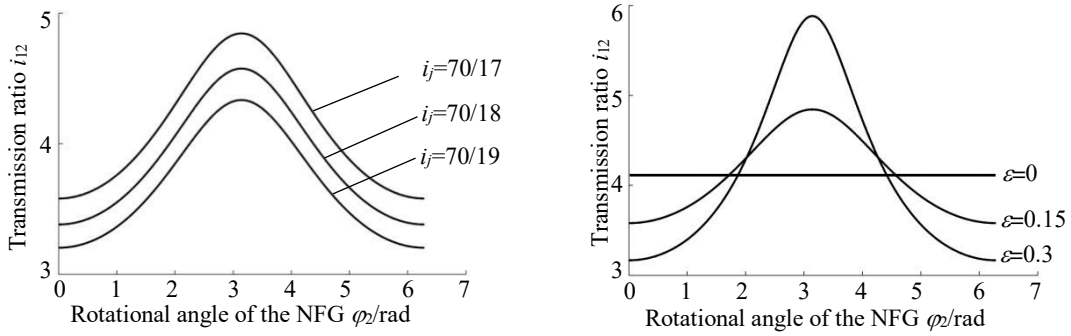

(a) Effect of i_j on the transmission ratio (b) Effect of ε on the transmission ratio

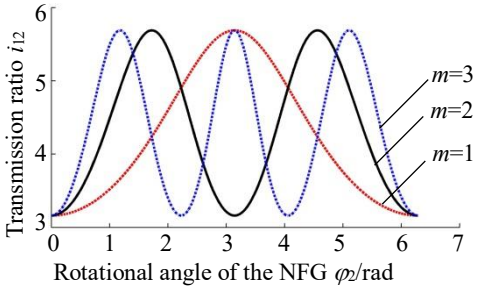

(b) Effect of m on the transmission ratio

Fig. 12 Transmission ratio with different design parameters

Thereby, it can be concluded that the reduction ratio, transmission range and number of the transmission ratio period of the NFG drive can be controlled by i_j, ε and m independently. However, for ordinary closed noncircular gears, the reduction ratio (the ratio of the number of the teeth between the two noncircular gears) must be equal to the ratio of orders of their pitch curves. In this case, the number of the transmission ratio period is associated with the reduction ratio. For example, the reduction ratio of the noncircular gears is 3/2 in Fig. 13, which is equal to the ratio of orders of the two gears. Correspondingly, the number of the transmission ratio period is 3 when the driven gear rotates a revolution. If the number of the transmission ratio period in Fig. 13 is changed to 4, then reduction ratio of the noncircular gears will be 2. By comparison, the features of the transmission ratio of the NFG are decided by specific parameters independently, which provides huge advantage of flexibility over other noncircular gears in design.

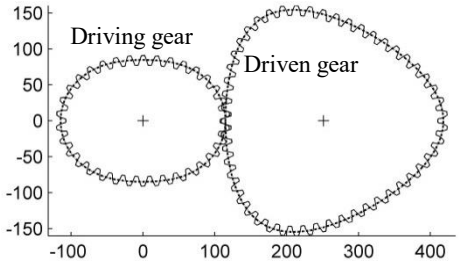

Fig. 13 Ordinary high-order noncircular gears

5.2 Simulation modelling

Two approaches are used to construct the tooth surfaces of the NFG with the design parameters in Table.1. One is to build a NFG model through simulating the machining process by a shaper in a CAD software. The shaper is replaced by a straight involute gear with m=2mm, α_0=20 ≡ and Z_s=20, and the wheel blank of the NFG is built according to its tooth width B_2 and addendum, which are shown in Fig. 14 (a). Let the shaper rotate relative to the wheel blank. After each rotation, the subtraction Boolean operation is performed between the wheel black and the shaper to simulate the gear shaping, as shown in Fig. 14 (b). If the rotational angle of the shaper is ϕ_s, the rotation angle of the wheel blank is calculated by

$$\phi_2 = \frac{\phi_s}{i_{js}} + \varepsilon \sin(\frac{\phi_s}{i_{js}}) \tag{22}$$

where $i_{js} = Z_2 / Z_s$. When the wheel blank turns one revolution, the teeth of the NFG are generated by the shaper completely as shown in Fig. 14(c).

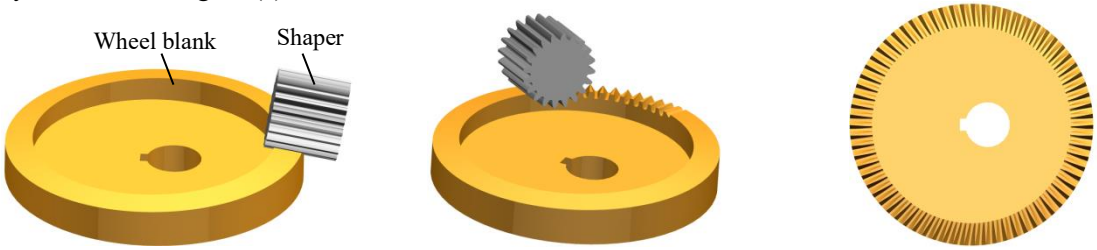

(a) Shaper and wheel blank (b) Gear cutting (c) NFG

Fig. 14 Simulation of machining process of the NFC

The other approach is to construct the tooth surface simulation model of the NFG by the presented mathematical equations. Using Eq. (13) and Eq. (17), we calculate the tooth surface data of the NFG. Then import those data into a 3-D graphics software to generate the tooth surfaces by the surface fitting function. A tooth model of the NFG is given in Fig. 15, where the solid curves on the left and right side of the tooth are the meshing lines between the NFG and the shaper, and the dashed curves are the intersecting line between the working and fillet

surfaces. By comparing the distribution of the meshing lines on the tooth surfaces, we can find that the left and right tooth surfaces of a tooth on the NFG are asymmetric, which exists on the other teeth too. Thereby, the meshing behaviors of the NFG drive are different when the cylindrical gear rotates clockwise and anticlockwise.

(a) Left tooth surface (b) Right tooth surface

Fig. 15 A tooth of the NFG generated by the tooth surface data

Then, the data of some of the meshing lines in Fig. 15 are imported to the 3-D software, where a comparison between the tooth surfaces by mathematical calculation and by simulation is made. Fig. 16 shows a solid tooth constructed by machining simulation and the tooth surface curves calculated by the mathematical model. It can be observed that the curves agree well with the tooth surface. The same results appear on other teeth of the NFG, which proves the correctness of the presented mathematical model of the NFG with intersecting axes.

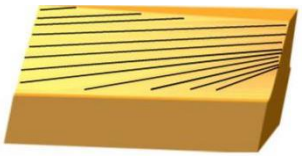

Fig. 16 Comparison of the tooth surfaces generated by the two modeling approaches

5.3 Transmission test

Although the solid model of the NFG can be constructed rapidly by the shaping simulation, its tooth surface comprises of many small discontinuous surfaces generated by gear cutting, which lead to great difficulty on kinematical simulation and generation of the CNC programs. Hence, we use the second method to construct the 3-D model of the NFG for the further manufacture. Fig. 17(a) illustrates the simulation model of the NFG and the cylindrical gear. Using the 3-D model of the NFG in Fig. 17(a), the NFG sample is machined by 3-axis CNC milling, which is shown in Fig. 17(b) and (c).

(a) Simulation model (b) Noncircular face gear (c) NFG and cylindrical gear

Fig. 17 NFG processed by a 3-axis CNC milling machine

Let the cylinder gear rotate at a constant speed and the load on the NFG be empty. The practical rotation speed of the NFG is tested by an optical encoder. Through further calculation, the practical transmission ratio of the NFG drive is obtained, which is compared with the theoretical transmission ratio in Fig. 15. The theoretical and experimental results agree with each other basically. The transmission error may result from the errors of simulation model, manufacture, installation and test. Considering the complex tooth surfaces of the NFG, we think the manufacture error is the main factor affecting the transmission accuracy of the NFG drive. The experimental results verify the feasibility of transmission of the NFG drive with intersecting axes and the correctness of its design method.

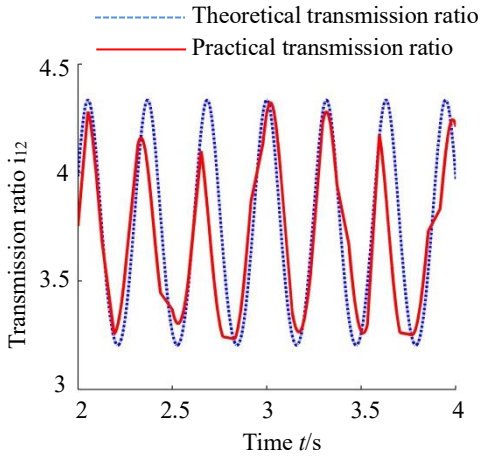

Fig. 18 Comparison of theoretical transmission ratio with practical transmission ratio

6 Conclusion

Noncircular face gear drive breaks the matching pattern of the traditional noncircular gears, which is a new type of variable transmission ratio gear mechanism composed of a cylindrical gear and a noncircular face gear. Aiming at the NFG with intersecting shafts, we investigate the construction of the pitch curves, the generation of the tooth surfaces and the features of the transmission rules and obtain the following conclusions:

(1) The generalized transmission ratio functions of the noncircular face gear are proposed based on Fourier series, which can be used to construct the closed pitch curves of noncircular face gears with intersecting shafts conveniently.

(2) The mathematical model of the tooth surfaces of the noncircular face gear with intersecting shafts is established by spatial meshing theory, which is verified by the machining simulation. The model lays the theoretical foundation for the contact analysis, the dynamic simulation and the manufacture of the noncircular face gear.

(3) The noncircular face gear drive can replace a serial gear mechanism with a pair of circular gears and a pair of noncircular gears in practice to light weight and reduce installation space.

(4) The reduction ratio, transmission range and number of transmission ratio period of the noncircular face gear drive can be controlled independently, which lead to great flexibility in design relative to the traditional noncircular gear.

Acknowledgment

The authors sincerely thank to Professor Tingzhi Ren of Yanshan University for his critical discussion and reading during manuscript preparation.

Authors' contributions

Dawei Liu was in charge of the whole research; Zhenzhen Lv wrote the manuscript; Guohao Zhao carried out the experiment. All authors read and approved the final manuscript.

Authors' information

Dawei Liu, born in 1984, is currently an associate professor at College of Mechanical Engineering, Yanshan University, China. He received his PhD degree from Yanshan University, China, in 2013. His research interests include noncircular gears and specialized robots.

Funding

Supported by National Natural Science Foundation of China (Grant No. 51705444) and Science and Technology Research Project of Hebei University (Grant No. QN2020266).

Competing interests

The authors declare no competing financial interests.

Reference

[1] E. Ottaviano, D. Mundo, G. A. Danieli, et al. Numerical and experimental analysis of non-circular gears and cam-follower systems as function generators. Mechanism and Machine Theory, 2008, 43(8):996-1008.

[2] J. W. Suh, K. Y. Kim. Harmonious cable actuation mechanism for soft robot joints using a pair of noncircular pulleys. Journal of Mechanisms and Robotics, 2018, 10(6): 061002.

[3] G. H. Xu, J. N. Chen, H.C. Zhao. Numerical Calculation and experiment of coupled dynamics of the differential velocity vane pump driven by the hybrid higher-order Fourier non-circular gears. Journal of Thermal Science, 2018, 27(3): 285-293.

[4] F. Y. Zheng, L. Hua, X. G. Han, et al.. Synthesis of indexing mechanisms with non-circular gears [J]. Mechanism and Machine Theory, 2016, 105: 108-128.
[5] M. L. Zhou, X. L. Xue,M. B. Qian, et al.. Optimal design and experiment of potted vegetable seedling Transplanting Mechanism with Punching Hole. Transactions of the Chinese Society for Agricultural Machinery, 2020, 51(01): 77-83.
[6] H. Z. Song, J. G. Zheng, W. Shi, et al.. Design and research of variable speed device based on spiral noncircular gear. Journal of Mechanical Engineering, 2017, 53(23): 101-107.
[7] J. M. Jia, B. Gao, W. L. Suo,et al.. Study on a new type of differential with variable ratio for off-road vehicles. China Mechanical Engineering, 2012, 23(023): 2844-2847.
[8] D. W. Liu, T. Z. Ren. Study on deformed limacon gear and motion optimization of its serial mechanism. J Mech Des, Trans ASME, 2011, 133(6): 061004.
[9] H. F. Quintero Riaza, S. Cardona Foix, L. Jordi Nebot. The synthesis of an N-lobe noncircular gear using Bézier and B-spline nonparametric curves in the design of its displacement law. J Mech Des, Trans ASME, 2007, 129(9): 981-985.
[10] G. H. Xu, J. N. Chen,G. F. Zhang. Design and performance analysis of Fourier non-circular gear-driven differential pump. Transactions of the Chinese Society for Agricultural Machinery, 2014, 45(12):80-87.
[11] Y. Wang, J. N. Chen, X. C. Sun. Parameter optimization and experimrnt of planting mechanism driven by planetary non-circular gears. Transactions of the Chinese Society for Agricultural Machinery, 2015, 46(09): 85-93.
[12] G. H. Xu, W. Liu, R. S. Xie. Design and experiment of six-blade differential pump driven by denatured higher order ratio Fourier non-circular gear pairs. Transactions of the Chinese Society for Agricultural Machinery, 2019, 050(002): 384-392.
[13] G. H. Xu, J. N. Chen, Z. P. Tong, Multi-objective optimization of mixed high-order Fourier non-circular gear-driven differential pump. Transactions of the Chinese Society for Agricultural Machinery, 2016, 47(001):383-390.
[14] D. W. Liu, T. Z. Ren. Creating pitch curve of closed noncircular gear by compensation method. Journal of Mechanical Engineering, 2011, 47(13), 147-152.
[15] F. L. Litvin, I. Gonzalez-Perez, K. Yukishima, et al. Generation of planar and helical elliptical gears by application of rack-cutter, hob and shaper. Computer Methods in Applied Mechanics and Engineering, 2007, 196(41-44): 4321-4336.
[16] J. Q. Xia, Y. Y.Liu, C. M. Geng, et al.. Non-circular bevel gear transmission with intersecting axes. J Mech Des, Trans ASME, 2008, 130(5): 1-6.
[17] K. Shi, J. Q. Xia, C. J. Wang. Design of noncircular bevel gear with concave pitch curve. Proc. Inst. Mech. Eng. Part C J. Mech. Eng. Sci., 2012, 227(3): 542-553.
[18] C. Lin, Y. J. Hou, H. Gong, et al.. Design and analysis of transmission mode for high-order deformed elliptic bevel gears. Journal of Mechanical Engineering, 2011, 47(13): 131-139.
[19] G. Figliolini, J. Angeles. Synthesis of the pitch cones of N-lobed elliptical bevel gears. Journal of Mechanical Design, Transactions of the ASME, 2011, 133(3): 031002.
[20] C. Lin, C. J. He. Tooth contact analysis of elliptical bevel gear with different misalignment. Proc. Inst. Mech. Eng. Part C J. Mech. Eng. Sci., 2019, 233(7): 2516-2525.
[21] C. Lin, Z. Q. Cai, X. Y. Wu, et al.. Transmission Mode for Curve-face Gear Pair [J]. Journal of Mechanical Engineering, 2018, 232(13): 2458-2468.
[22] C. Lin, H. Gong, G. Nie, et al.. Geometry design three-dimensional modeling and kinematic analysis of orthogonal fluctuating gear ratio face gear drive. Proc. Inst. Mech. Eng. Part C J. Mech. Eng. Sci., 2013, 227(4): 779-773.
[23] C. Lin, C. J. He, Y. A. Hu. Analysis on the kinematical characteristics of compound motion curve-face gear pair [J]. Mechanism and Machine Theory, 2018, 128: 298-313.
[24] C. Lin, C. J. He. Analysis of tooth contact and transmission errors of curve-face gear. Proc. Inst. Mech. Eng. Part C J. Mech. Eng. Sci., 2017, 231(19): 3579-3589.
[25] D. W. Liu, T. Z. Ren, X. Jin. Meshing theory of speed integration gear. Journal of Mechanical Engineering, 2016, 52(15): 1-7.
[26] D. W. Liu, G. H. Wang, T. Z. Ren. Transmission principle and Geometrical model of Eccentric Face Gear. Mechanism and Machine Theory, 2017, 109: 51-64.
[27] F. Litvin. Gear geometry and applied theory, Englewood Cliffs, NJ: Prentice-Hall, 1994.

Figures

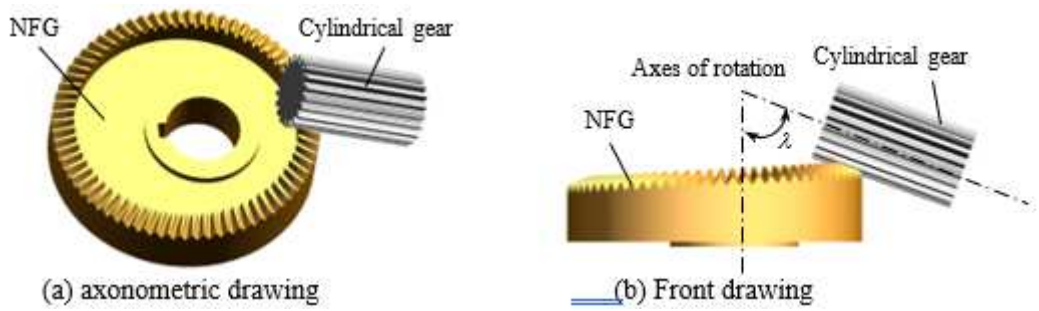

Figure 1

Noncircular face gear drive

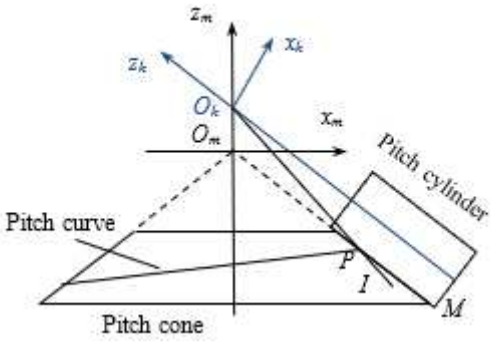

Figure 2

Pitch surface and pitch curve

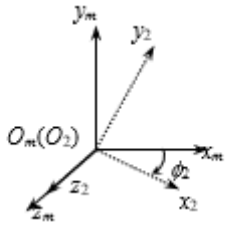

Figure 3

Relationships between S2 and Sm

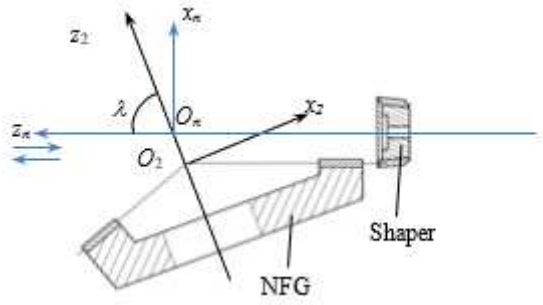

Figure 4

Generation of the NFG by a shaper

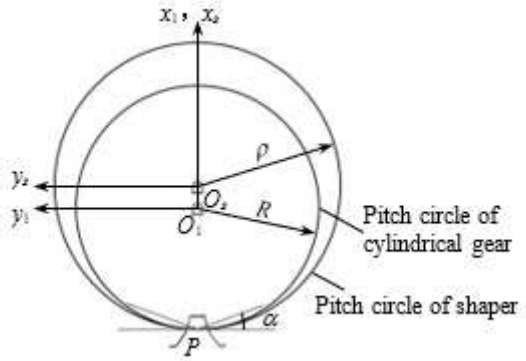

Figure 5

Relationship between the shaper and the cylindrical gear

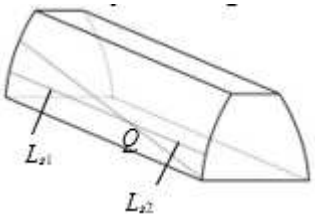

Figure 6

Contacting lines on the tooth of the shaper cutter

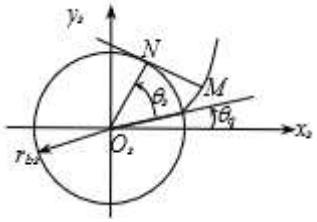

Figure 7

Tooth profile of the shaper

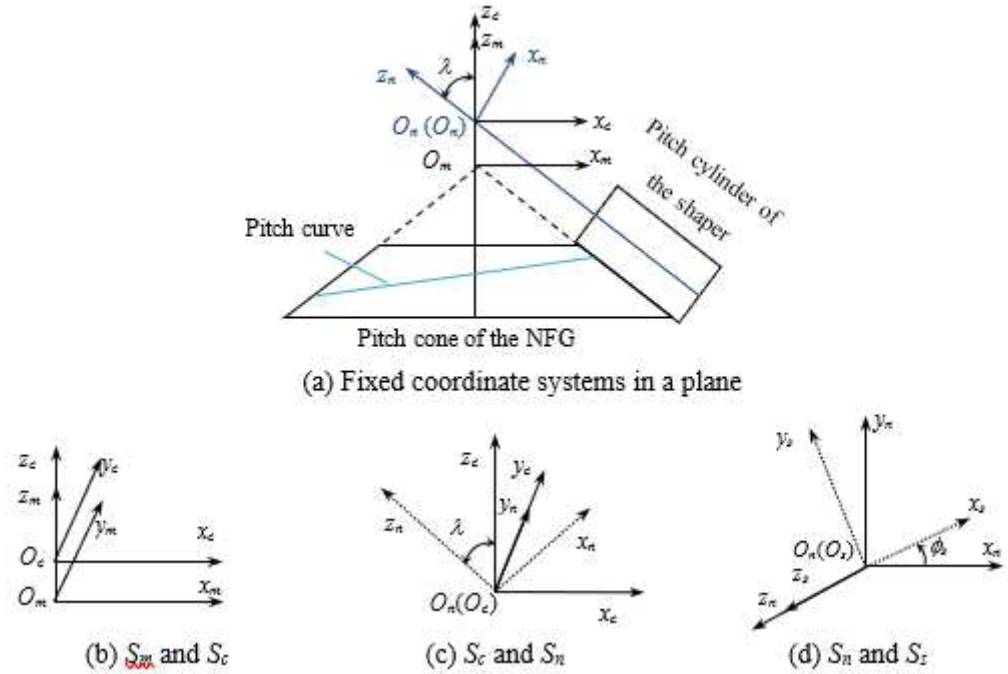

Figure 8

Relationships of coordinate systems

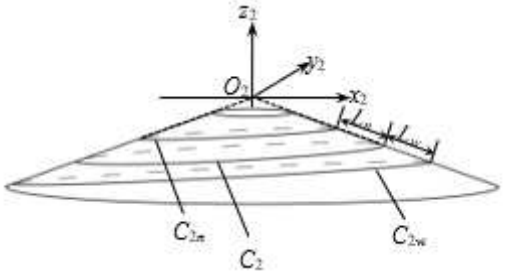

Figure 9

Inner and outer curve of the teeth on the pitch cone

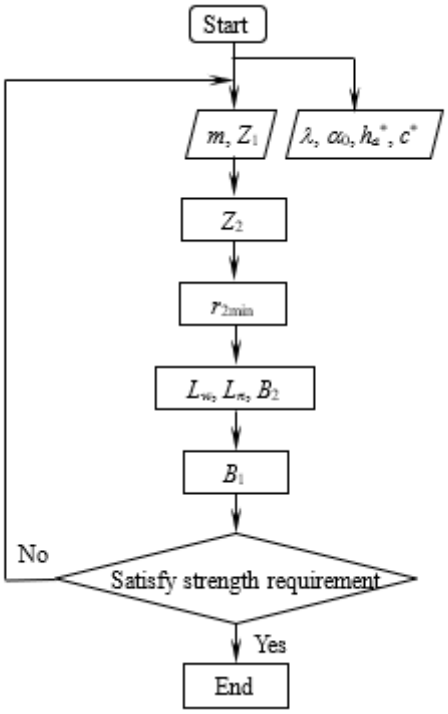

Figure 10

Design flow of the NFG drive

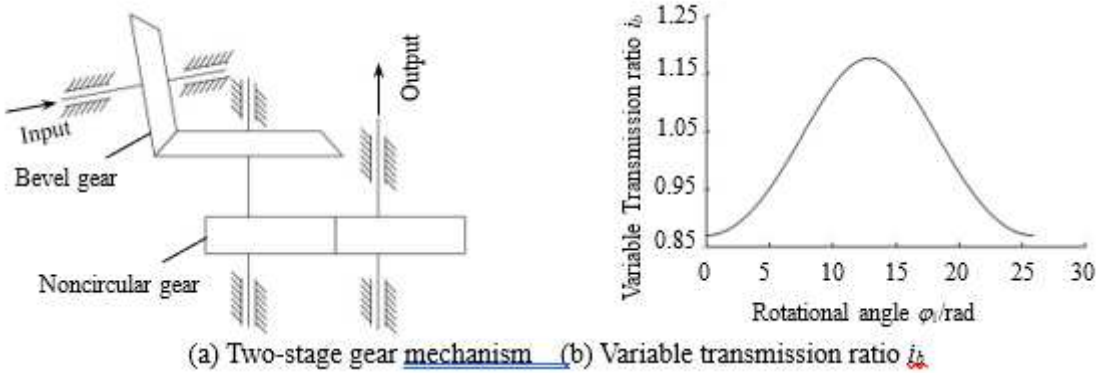

(a) Two-stage gear mechanism (b) Variable transmission ratio i_b

Figure 11

Equivalent transmission mechanism of the NFG drive

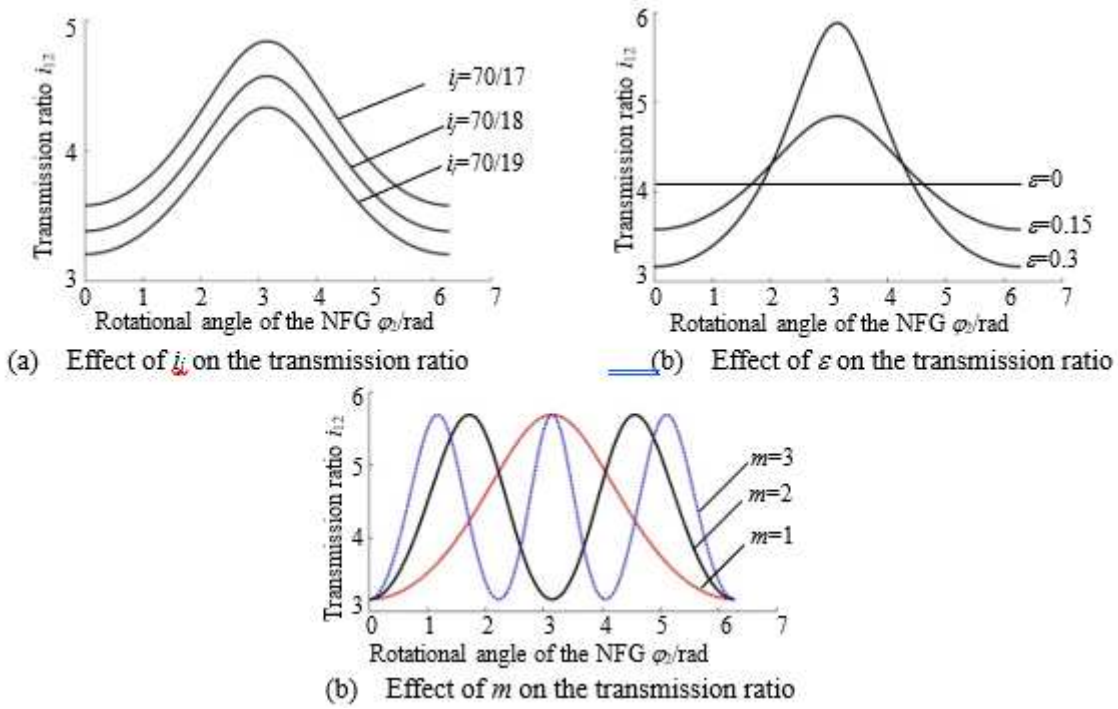

Figure 12

Transmission ratio with different design parameters

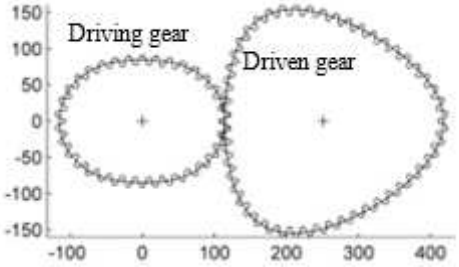

Figure 13

Ordinary high-order noncircular gears

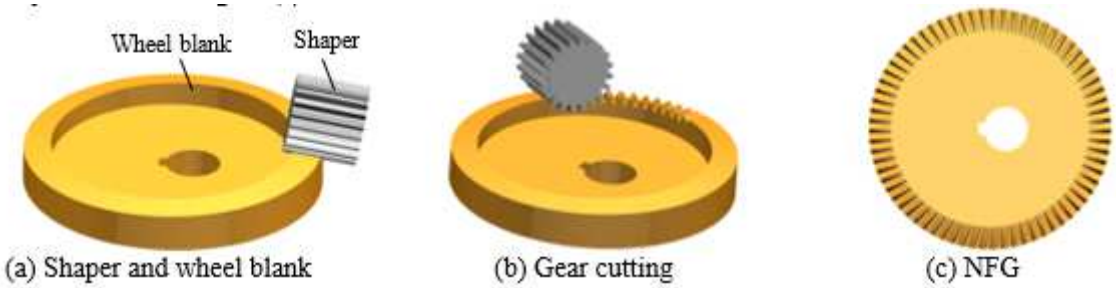

Figure 14

Simulation of machining process of the NFC

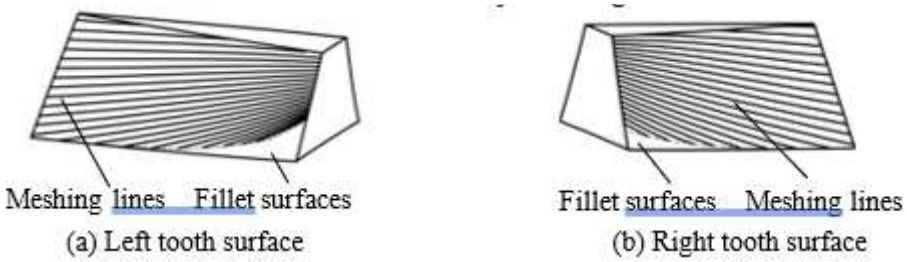

Figure 15

A tooth of the NFG generated by the tooth surface data

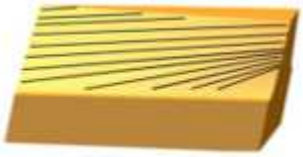

Figure 16

Comparison of the tooth surfaces generated by the two modeling approaches

Figure 17

NFG processed by a 3-axis CNC milling machine

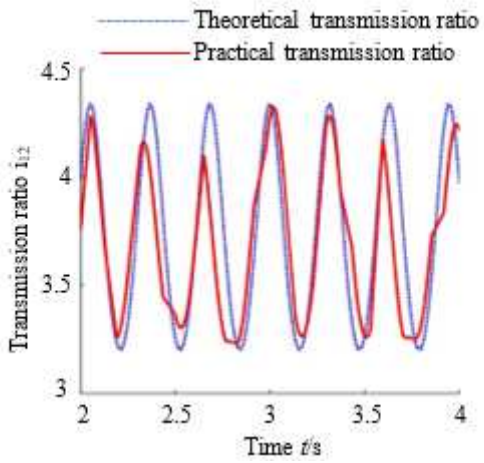

Figure 18

Comparison of theoretical transmission ratio with practical transmission ratio